Mechanism of Impact Pressure Generation from Spark-Generated Bubble Collapse Near a Wall

A. Shima,* K. Takayama,† and Y. Tomita‡
Tohoku University, Sendai, Japan
and
N. Ohsawa§
Toshiba Engineering Company, Tokyo, Japan

This paper deals with a detailed experimental investigation on the collapse of a single spark-generated bubble near a solid wall and the mechanism of its induced impact pressure generation. By changing L/R_{max} from 0.14 to 17.1, where L is the distance between the electrodes and the solid wall and R_{max} a maximum bubble radius, the collapse of the bubble was observed with an Ima-Con high speed camera and, simultaneously, the induced impact wall pressure was measured. Consequently, the induced impact wall pressure history revealed that three types of the bubble collapse modes exist depending on L/R_{max}; i.e., the region where a shock wave is dominant to the impact wall pressure at $L/R_{max} \lesssim 0.3$ and $\gtrsim 1.5$, a liquid jet at $0.6 \lesssim L/R_{max} \lesssim 0.8$, and both a shock wave and a liquid jet at $0.3 \lesssim L/R_{max} \lesssim 0.6$ and $0.8 \lesssim L/R_{max} \lesssim 1.5$.

Introduction

ONCE the cavitation phenomenon takes place in hydraulic machines their performances are drastically reduced and undesirable phenomena are induced. From a practical point of view, the erosion of the material exposed to the cavitation is one of the most serious problems. Therefore, it is of primary importance to understand the mechanism of the cavitation erosion phenomenon.

Knapp[1] obtained a relationship between the features of the cavitation occurring on a hemispherical model surface and the erosion-pit distribution over the model surface, and showed that the most serious erosion took place at the trailing edge of the cavity where the bubbles were collapsing. His observation indicated that the cavitation erosion is closely related to the process of the bubble collapse and demonstrated the necessity of investigating the mechanism of bubble collapse and its induced impact on wall pressure. For these reasons, a number of experimental[12-16] and theoretical[17-32] studies were done on the behavior of a single bubble in a quiescent liquid. At present two factors are found to predominate in generating the impact pressure at the bubble collapse; they are a liquid jet caused by instability of a collapsing bubble near the solid wall and a shock wave generated at re-expansion of a collapsing bubble. Unfortunately, however, there is no definite experimental evidence to show which factor is most influential if the type of the cavitation is specified. In fact, by observing a metal surface suffering the cavitation erosion, Efimov et al.[33] showed that three types of damage forces are possible, depending on various stages of the developing cavitation: i.e., damage forces from a shock wave, from a microjet, and from the coexistence of a shock wave and a liquid jet. In order to establish the so-called scaling law necessary in designing actual hydraulic machines, Thiruvengadam[34] and Kato[35] presented a method to estimate the amount of cavitation erosion by assuming energy density distributions released from a shock-wave-type bubble collapse and a liquid-jet-type bubble collapse. However, in spite of the efforts of previous workers, many aspects of the cavitation erosion phenomenon are far from being understood completely.

Observing various stages of the growth and collapse of a single spark-generated bubble with an Ima-Con high speed camera, in a previous report the authors[16] clarified the effect of the wall on the bubble collapse in detail. The mechanism of a bubble collapse is found to be dependent totally on the distance L between the electrodes and the solid wall and a maximum bubble radius R_{max} and the condition of the bubble attached to the wall. The present study is an extension of the previous work in order to provide physically a more rigorous explanation of the mechanism of the collapse of a spark-generated bubble near a solid wall by measuring the impact wall-pressure history, which was not done in the previous study. From both the pressure measurement and the high-speed sequential photographs of a single spark-generated bubble collapse, it is revealed that, depending on a parameter L/R_{max}, there are regions where the impact wall pressure is generated primarily by a shock wave, by a liquid jet, and by cooperation of both a shock wave and a liquid jet.

Experiments

A schematic diagram of the experimental setup is shown in Fig. 1. A $300 \times 240 \times 240$-mm stainless steel bubble chamber with 100-mm-diam observation windows was used. About 15 liters of tap water at room temperature was added to the chamber. At the center of the chamber 0.3-mm-diam tungsten electrodes were set in a line. The gap distance of the electrodes was determined precisely by means of a micrometer from outside the chamber. As shown in Fig. 1, underneath the gap, a 50-mm-diam brass disk was placed at the center of which a calibrated pressure transducer (Swiss Kistler model 603B, characteristic frequency 400 kHz, accuracy 0.5 kPa and a maximum pressure 25 MPa) was mounted flush to the disk surface. The rise time of this pressure transducer to the stepwise pressure jump is about 1 μs, fast enough to detect the shock wave in water. The arrangement of the disk to the electrodes, as well as the optical alignment, were done with a He-Ne laser. A condenser bank of $C = 0.5$ μF and charge voltage V_c up to 10 kV (i.e., charge energy $E_c = 25$ J) was used, and both the discharge current and the discharge voltage were monitored for each run.

Received June 17, 1981; revision received Feb. 5, 1982.

*Professor, Institute of High Speed Mechanics.
†Assistant Professor, Institute of High Speed Mechanics. Member AIAA.
‡Research Assistant, Institute of High Speed Mechanics.
§Engineer.

The motion of a single spark-generated bubble was observed by means of an Ima-Con high speed camera (John Hadland 700) and a light source of argon-ion laser (NEC GLG3200, 2 W) equipped with a 1-ms opening duration mechanical shutter. The framing speed of the high-speed camera was 200,000 frames/s. Output signals from the pressure transducer were displayed on an oscilloscope or an X-Y recorder through a transient recorder (Iwatsu DM 901, 25 MHz). A block diagram of the experimental method is also shown in Fig. 1 and is self-explanatory. As shown in Fig. 1, a discharge current at the bubble initiation was used as a trigger signal to start the measuring system. In the present experiment, the condenser bank was equipped with a main gap switch which was operated by the external trigger signal (see Ref. 16 for details).

All of the measurements were conducted with constant R_{max}. In order to realize this constant maximum bubble radius, preparatory experiments were done. If R_{max} were measured successively without changing the electrodes but with the charge energy kept constant for each run, the gap distance l_d might be varied and, consequently, R_{max} changed. Figure 2 shows the relationship between N_s and R_{max}, where N_s designates the number of successive discharges. As shown in Fig. 2, for $N_s \gtrsim 10$ there is a region where R_{max} is almost constant. Therefore, we decided to use this stable region for experiment. By using these procedures, we could determine R_{max} fairly accurately simply by controlling E_c. Figure 3 shows the relationship between R_{max} and E_c.

Since the experiments were conducted for a specified value of L/R_{max}, two schemes were possible; 1) R_{max} = const and L variable and 2) L = const and R_{max} variable. In the present experiment, the following values were used: in case 1, R_{max} = 3.5 mm (i.e., V_c = 3.0 kV) and $L = 0.5 \sim 60$ ($L/R_{max} = 0.14 \sim 17.1$); and in case 2, L = 3.0 mm and $R_{max} = 2.5 \sim 6.0$ mm ($L/R_{max} = 0.5 \sim 1.2$) and L = 5 mm and $R_{max} = 2.3 \sim 8.3$ mm ($L/R_{max} = 0.6 \sim 2.2$). A good reproducibility for L/R_{max} was obtained for each run.

Results and Discussion

Case 1, fixed R_{max} = 3.5 mm and variable L, is discussed first. The typical impact wall pressure histories are shown in Figs. 4a-d for various values of L. Abscissas are time marching from right to left and ordinates the pressure in MPa. Figure 5 shows the relationship between a maximum impact wall pressure p_{max} and L/R_{max}. Open circles show averaged values from 10 experimental data points with the same initial conditions. For $L/R_{max} = 0.14$, 1, and 10, p_{max} = 20, 10, and 1 MPa, respectively. It is noted that for $L/R_{max} = 3.0$, p_{max} = 4 MPa, and this value is almost the same as Teslenko's experimental data of a laser-induced bubble.[13] For $L/R_{max} \gtrsim 1.0$, p_{max} decreases monotonically with increasing L and for $L/R_{max} \gtrsim 3.0$, the p_{max} curve agrees with a $1/L$ decrease. This means that the maximum pressure at L measured from the center of the collapsing bubble decreases proportionally with $1/L$. The region where p_{max} decreases with $1/L$ is consistent with a theoretically predicted region.[17,20] Therefore by extrapolating the p_{max} curve along a $1/L$ decrease curve up to 0.2 mm (which is equivalent to a final minimum radius of the collapsing bubble at $L \to \infty$) we can estimate a final maximum pressure of a collapsing bubble to be about 200 MPa. In the present experiment, the authors reconfirmed the shock wave generation for a larger L case, and from high-speed photographs and simultaneously measured wall pressure histories, a maximum impact wall pressure was measured at the moment where the shock wave just collided against the wall. It is concluded that for a larger L/R_{max} case the main impact wall pressure source is a shock wave generated at the first re-expansion of the bubble.

For $L/R_{max} \lesssim 3.0$, since a collapsing bubble departs from spherical shape, the p_{max} curve in Fig. 5 deviates from the $1/L$ decrease curve. For $L/R_{max} < 1.0$, where a bubble collapses

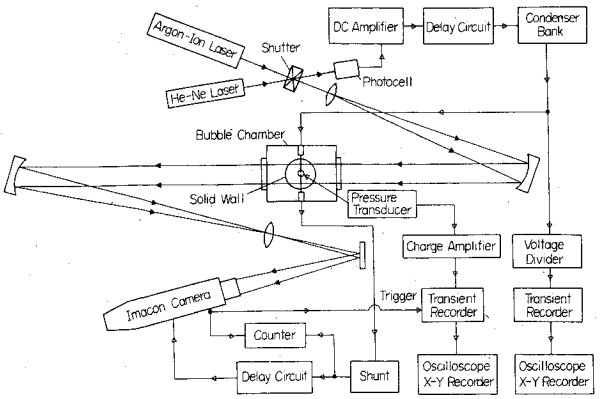

Fig. 1 Block diagram of the experimental apparatus.

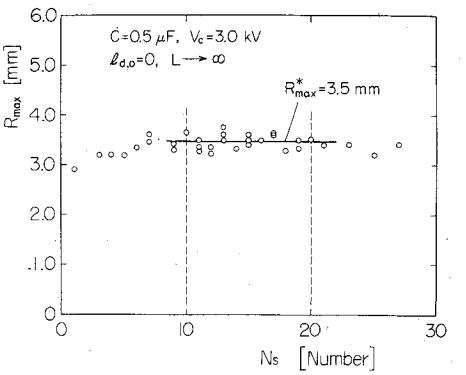

Fig. 2 Relationship between the maximum bubble radius R_{max} and the number of serial spark discharges N_s.

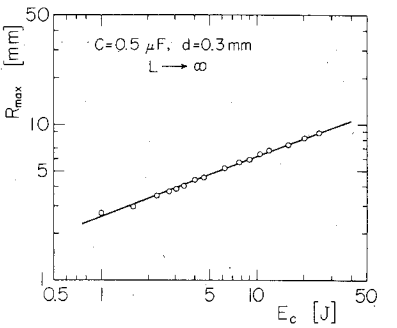

Fig. 3 Relationship between the maximum bubble radius R_{max} and the charge energy E_c.

with some parts touching the wall, p_{max} sharply decreases to a minimum. Whereas with a decreasing L/R_{max}, p_{max} begins to increase again and for $L/R_{max} \lesssim 0.4$, the p_{max} curve apparently lies on a curve being extrapolated from a curve drawn for a larger L/R_{max}.

Let the measured pressure rise time in $L/R_{max} = 10$ case be $\Delta\tau_0$, which corresponds to the rise time of the pressure transducer used in the present experiment against a pressure jump of a shock wave having propagated from a distance. A dimensionless rise time $C^* = \Delta\tau_0/\Delta\tau$ for various L/R_{max} is plotted in Fig. 6, where each point is an average from 10 experimental data points with the same initial conditions. For both $L/R_{max} \gtrsim 1.5$ and $\lesssim 0.3$, $C^* \gtrsim 1$. This shows that the steep pressure rise is due to a shock wave as the pressure source. For $1.5 \lesssim L/R_{max} \lesssim 3.0$, high-speed shadowgraphs revealed that a bubble slowly moved toward the wall, collapsed, and then clearly generated a shock wave. However, the previous study[16] showed that in this region a liquid jet

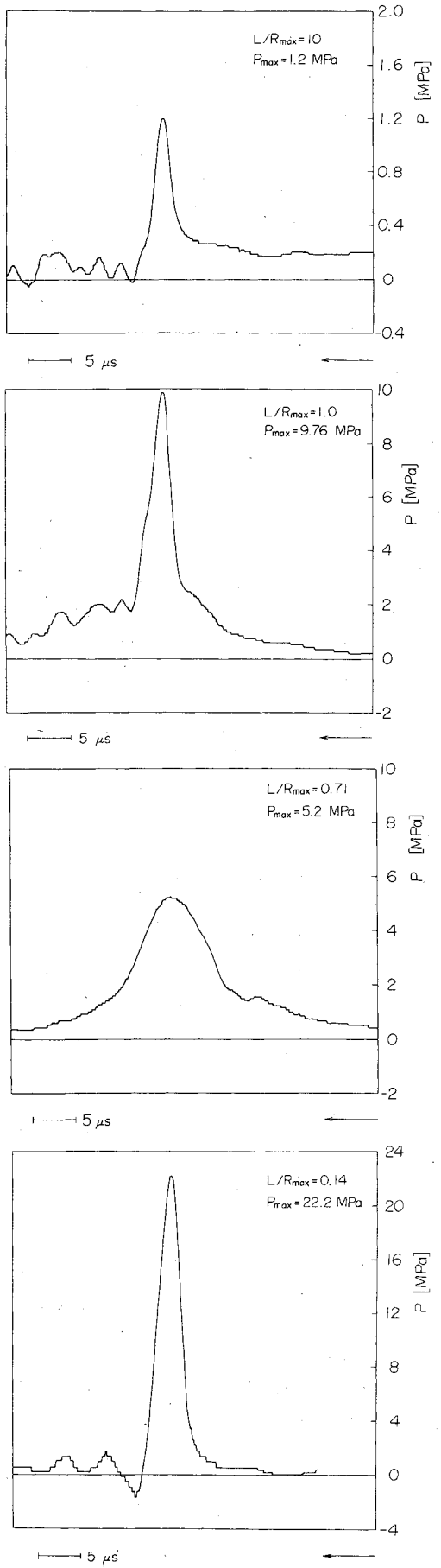

Fig. 4 Typical impact wall pressure histories, $R_{max}=3.5$ mm; a) $L=35$ mm ($L/R_{max}=10.0$), b) $L=3.5$ mm ($L/R_{max}=1.0$), c) $L=2.5$ mm ($L/R_{max}=0.71$), and d) $L=0.5$ mm ($L/R_{max}=0.14$).

could not reach the wall. For $L/R_{max} \lesssim 0.3$, an attached bubble with a maximum volume was nonhemispherical with an obtuse contact angle to the wall. Analyses using a potential theory[25,29] show that a shock wave is possible even in this case since when a bubble collapses some of the liquid near the wall is accelerated along the wall surface. In fact, it was observed that at the final stage of bubble collapse a strong shock wave was generated.[16]

As shown in Fig. 6, there is a minimum C^*, say $C^* \lesssim 0.5$, for $0.6 \lesssim L/R_{max} \lesssim 0.8$. In this region, the development of a liquid jet is clearly visible and, at the same time a number of wavelets are observed. However, since the energy possessed by a bubble is shared with the formation of wavelets and the liquid jet formation occurs too quickly for the wavelets to be accumulated into a shock wave, p_{max} is a minimum and the measured pressure rise time is a maximum. It is concluded that a slower pressure rise indicates that a liquid jet is the source of the impact wall pressure generation. Gibson and Aust[8] observed the motion of a collapsing single vapor bubble near the wall and determined the re-entrant jet velocity. They obtained the very interesting result that the maximum jet velocity occurs at $0.5 \lesssim L/R_{max} \lesssim 1.0$. Their result also supports the present conclusion.

In both the $0.3 \lesssim L/R_{max} \lesssim 0.6$ and $0.8 \lesssim L/R_{max} \lesssim 1.5$ regions, it is expected that both a shock wave and a liquid jet contribute equally to the impact pressure generation. The experimental evidence of cooperation between a shock wave and a liquid jet is shown in Fig. 7 for $L=3.8$ mm ($L/R_{max}=1.09$). In Fig. 7, the impact wall pressure history and the high-speed shadowgraphs are shown and arrowed numbers at the impact wall pressure history diagram correspond to the frame numbers of the simultaneously taken high-speed shadowgraphs. A liquid jet reaches the wall prior to the bubble collapse. Comparing high-speed shadowgraphs

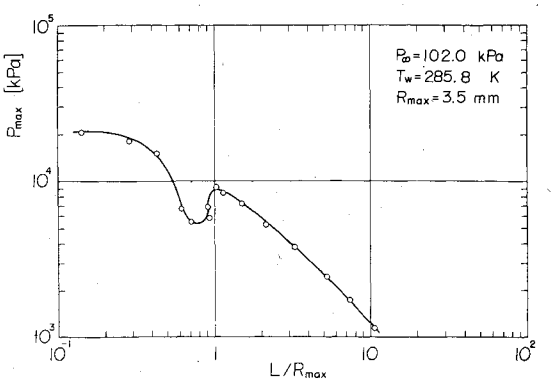

Fig. 5 Relationship between the maximum impact wall pressure p_{max} and the dimensionless distance L/R_{max} ($R_{max}=3.5$ mm).

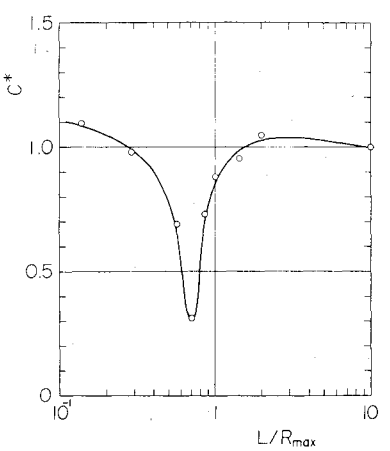

Fig. 6 Variation of the dimensionless rise time C^* with L/R_{max}.

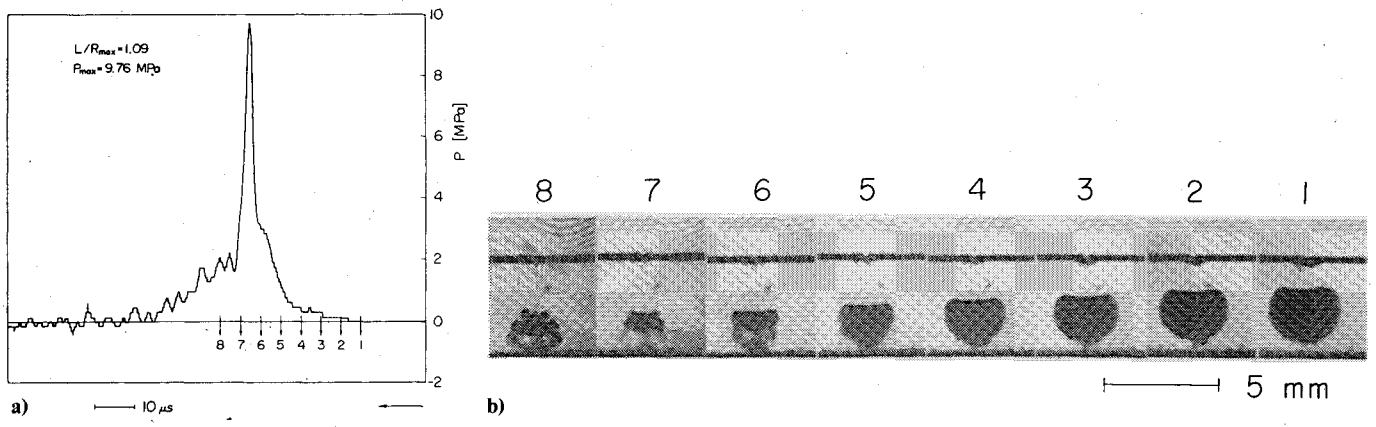

Fig. 7 Coexistence of a shock wave and a liquid jet, $R_{max}=3.5$ mm, $L=3.8$ mm, $L/R_{max}=1.09$; a) impact wall pressure history and b) shadowgraphs.

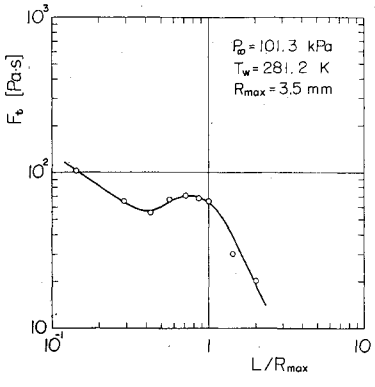

Fig. 8 Variation of the impulse F_t with L/R_{max}, $R_{max}=3.5$ mm.

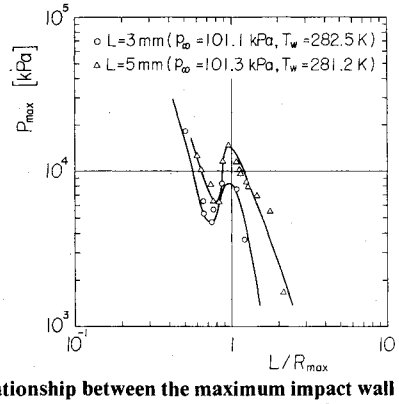

Fig. 9 Relationship between the maximum impact wall pressure p_{max} and the dimensionless distance L/R_{max}; o: $L=3$ mm, Δ: $L=5$ mm.

with the impact wall pressure history, it is found that there is first a slow pressure rise due to a contribution from a liquid jet and, next, a steep pressure rise corresponding to a contribution from a shock wave. It should be mentioned here that the pressure transducer used in the present experiment has a diameter of 5.55 mm, which is fairly larger than the size of an actual liquid jet. The maximum impact wall pressure released from the liquid jet was expected to be very high, since the measured value is one averaged over the diameter of the pressure transducer. More direct and accurate methods of measuring the local pressure should be developed in future investigations.

Figure 8 shows the relation between the impulse

$$F_t=\int_0^t p\,dt$$

and L/R_{max}. For $L/R_{max}>1.0$, F_t decreases along the $1/L^2$ curve and for $0.3<L/R_{max}<1.0$, F_t drops down to a minimum but not as drastically as seen in Fig. 5 for the p_{max} case. This indicates that the total energy released by a bubble collapse is invariant independent of the sources and types of impact wall pressure. It is, therefore, expected that the closer to the wall a bubble collapses, the larger the amount of energy released. This means that the chance of more serious erosion appearing increases when a bubble collapses closer to the wall.

The second case, i.e., constant L and variable R_{max}, is discussed here. As mentioned above R_{max} is changeable by controlling the input charge energy E_c. For $L=3.0$ mm and 5.0 mm, the relationship between p_{max} and L/R_{max} is shown in Fig. 9. The general tendency of p_{max} vs L/R_{max} is similar in both the $L=3.0$ and 5.0 mm cases. Analogously, as in Fig. 5, p_{max} is a minimum at $L/R_{max}=0.7\sim0.8$. It is obvious that the maximum impact wall pressure is described by a parameter L/R_{max} and the region in which the type of the impact wall pressure source is specified can also be determined only by L/R_{max}.

Conclusions

In order to clarify the mechanism of the collapse and induced impact wall pressure generation of a single spark-generated bubble, a detailed experiment was conducted by means of high-speed photography and pressure measurement. The results obtained are summarized as follows:

1) The source of the impact pressure at the solid wall was classified into three types, depending on L/R_{max}. The type and the region of their existence are a) the region where a shock wave is dominant, at $L/R_{max}\lesssim0.3$ and $\gtrsim1.5$; b) the region where a liquid jet is dominant, at $0.6\lesssim L/R_{max}\lesssim0.8$; and c) the region where a shock wave and a liquid jet coexist, at $0.3\lesssim L/R_{max}\lesssim0.6$, and $0.8\lesssim L/R_{max}\lesssim1.5$.

2) The impulse F_t received at the wall is larger for a bubble closer to the wall or that attached to the wall. F_t changed slightly for $L/R_{max}<1.0$ and the total amount of the energy released by a collapsing bubble is almost invariant. The type of energy release transforms with L/R_{max} decreasing as follows: shock wave→liquid jet→shock wave.

3) The $p_{max}-L/R_{max}$ curve has a minimum at $L/R_{max}\simeq0.6$ to 0.8 in both $R_{max}=$const and L variable and $L=$const and R_{max} variable cases. The mechanism of the impact wall pressure generation is strongly dependent on a parameter L/R_{max}.

Acknowledgments

The authors would like to express their thanks to the late Professor Emeritus F. Numachi of Tohoku University for his encouragement throughout the course of the present study. The authors also wish to express their appreciation to Professor M. Honda, Director of the Institute of High Speed

Mechanics, Tohoku University for his advice and comments on the present study. The authors are indebted to N. Miura for the artwork and S. Takasaki and Y. Nishiuchi for typing the manuscript. The present project was financially supported by a Science and Research Grant in Aid offered by Ministry of Education in 1980.

References

[1] Knapp, R. T., "Recent Investigations of the Mechanics of Cavitation and Cavitation Damage," *Transactions of ASME*, Vol. 77, Oct. 1955, pp. 1045-1054.

[2] Harrison, M., "An Experimental Study of Single Bubble Cavitation Noise," *Journal of Acoustical Society of America*, Vol. 24, Nov. 1952, pp. 776-782.

[3] Mellen, R. H., "An Experimental Study of the Collapse of a Spherical Cavity in Water," *Journal of Acoustical Society of America*, Vol. 28, May 1956, pp. 447-454.

[4] Jones, I. R. and Edwards, D. H., "An Experimental Study of the Forces Generated by the Collapse of Transient Cavities in Water," *Journal of Fluid Mechanics*, Vol. 7, April 1960, pp. 596-609.

[5] Naudé, C. F. and Ellis, A. T., "On the Mechanism of Cavitation Damage by Nonhemispherical Cavities Collapsing in Contact with a Solid Boundary," *Journal of Basic Engineering, Transactions of ASME*, Ser. D, Vol. 83, Dec. 1961, pp. 648-656.

[6] Shutler, N. D. and Mesler, R. B., "A Photographic Study of the Dynamics and Damage Capabilities of Bubbles Collapsing Near Solid Boundaries," *Journal of Basic Engineering, Transactions of ASME*, Ser. D., Vol. 87, Sept. 1965, pp. 511-517.

[7] Ellis, A. T., "On Jets and Shock Waves from Cavitation," *Proceedings of Sixth Symposium on Naval Hydrodynamics*, Washington, D.C., 1966, pp. 137-161.

[8] Gibson, D. C and Aust, I. E., "Cavitation Adjacent to Plane Boundaries," *Conference on Hydraulics and Fluid Mechanics*, 1968, pp. 210-214.

[9] Kling, C. L. and Hammitt, F. G., "A Photographic Study of Spark-Induced Cavitation Bubble Collapse," *Journal of Basic Engineering, Transactions of ASME*, Ser. D, Vol. 94, Dec. 1972, pp. 825-833.

[10] Smith, R. H. and Mesler, R. B., "A Photographic Study of the Effect of an Air Bubble on the Growth and Collapse of a Vapor Bubble Near a Surface," *Journal of Basic Engineering, Transactions of ASME*, Ser. D, Vol. 94, Dec. 1972, pp. 933-942.

[11] Lauterborn, W., "Kavitation durch Laserlicht," *Acustica*, Vol. 31, 1974, pp. 51-78.

[12] Lauterborn, W. and Bolle, H., "Experimental Investigation of Cavitation-Bubble Collapse in Neighborhood of a Solid Boundary," *Journal of Fluid Mechanics*, Vol. 72, Nov. 1975, pp. 391-399.

[13] Teslenko, V. S., "Experimental Investigation of Bubble Collapse at Laser-Induced Breakdown in Liquids," *Cavitation and Inhomogeneities in Underwater Acoustics*, Vol. 4, edited by W. Lauterborn, Springer, Berlin, Heidelberg, New York, 1980, pp. 30-34.

[14] Ebeling, K. J., "Zum Verhalten kugelförmiger, lasererzeugter Kavitationsblase in Wasser," *Acustica*, Vol. 40, 1978, pp. 229-239.

[15] Fujikawa, S. and Akamatsu, T., "Experimental Investigations of Cavitation Bubble Collapse by a Water Shock Tube," *Bulletin of the Japan Society of Mechanical Engineers*, Vol. 21, Feb. 1978, pp. 223-230.

[16] Shima, A., Takayama, K., Tomita, Y., and Miura, N., "An Experimental Study on Effects of a Solid Wall on the Motion of Bubbles and Shock Waves in Bubble Collapse," *Acustica*, Vol. 48, 1981, pp. 293-301.

[17] Rattray, M. Jr., "Perturbation Effects in Cavitation Bubble Dynamics," Ph.D. Thesis, Institute of Technology, Pasadena, Calif., 1951.

[18] Hickling, R. and Plesset, M. S., "Collapse and Rebound of a Spherical Bubble in Water," *Physics of Fluids*, Vol. 7, Jan. 1964, pp. 7-14.

[19] Shima, A., "The Behavior of a Spherical Bubble in the Vicinity of a Solid Wall," *Journal of Basic Engineering, Transactions of ASME*, Ser. D, Vol. 90, March 1968, pp. 75-89.

[20] Shima, A., "The Behavior of a Spherical Bubble in the Vicinity of the Solid Wall (Report 4)," *Reports of Institute of High Speed Mechanics*, Tohoku University, Vol. 23, 1971, pp. 195-219.

[21] Plesset, M. S. and Chapman, R. B., "Collapse of an Initially Spherical Vapour Cavity in the Neighborhood of a Solid Boundary," *Journal of Fluid Mechanics*, Vol. 47, May 1971, pp. 283-290.

[22] Mitchell, T. M. and Hammitt, F. G., "Asymmetric Cavitation Bubble Collapse," *Journal of Basic Engineering, Transactions of ASME*, Ser. I, Vol. 95, March 1973, pp. 29-37.

[23] Shima, A. and Tomita, Y., "On the Impulse Pressure Accompanying Spherical Bubble Collapse in Liquids," *Reports of Institute of High Speed Mechanics*, Tohoku University, Vol. 31, 1975, pp. 97-135.

[24] Tomita, Y. and Shima, A., "On the Behavior of a Spherical Bubble and the Impulse Pressure in a Viscous Compressible Liquid," *Bulletin of the Japan Society of Mechanical Engineers*, Vol. 20, Nov. 1977, pp. 1453-1460.

[25] Shima, A. and Nakajima, K., "The Collapse of a Non-Hemispherical Bubble Attached to a Solid Wall," *Journal of Fluid Mechanics*, Vol. 80, April 1977, pp. 369-391.

[26] Nakajima, K. and Shima, A., "Analysis of the Behavior of a Bubble in a Viscous Incompressible Liquid by Finite Element Method," *Ingenieur-Archiv*, Bd. 46, 1977, pp. 21-34.

[27] Rath, H. J., "Zum Einfluss der Kompressibilität des Fluides bei sphärisch schwingenden Gasblasen un Flüssigkeiten," *Igenieur-Archiv*, Bd. 47, 1978, pp. 383-390.

[28] Tomita, Y. and Shima, A., "The Effects of Heat Transfer on the Behavior of a Bubble and the Impulse Pressure in a Viscous Compressible Liquid," *Zeitschrift für angewandte Mathematik und Mechanik*, Bd. 59, 1979, pp. 297-306.

[29] Shima, A. and Sato, Y., "The Collapse of a Bubble Attached to a Solid Wall," *Ingenieur-Archiv*, Bd. 48, 1979, pp. 85-95.

[30] Fujikawa, S. and Akamatsu, T., "Effects of the Non-Equilibrium Condensation of Vapour on the Pressure Wave Produced by the Collapse of a Bubble in a Liquid," *Journal of Fluid Mechanics*, Vol. 97, April 1980, pp. 481-512.

[31] Sato, Y. and Shima, A., "The Collapse of an Initially Spherical Bubble Near a Solid Wall," *Reports of Institute of High Speed Mechanics*, Tohoku University, Vol. 42, 1980, pp. 1-24.

[32] Shima, A. and Tomita, Y., "The Behavior of a Spherical Bubble Near a Solid Wall in Compressible Liquid," *Ingenieur-Archiv*, Bd. 51, 1981, pp. 243-255.

[33] Efimov, A. V., Vorobév, G. A., and Filenko, Yu. I., "Mechanism of Cavitation Damage and Structure of a Cavitation Eddy," *Proceedings of IAHR Symposium on Two-Phase Flow and Cavitation in Energy Production Systems*, Grenoble, 1976, pp. 159-169.

[34] Thiruvengadam, A., "Scaling Laws for Cavitation Erosion," *Proceedings of IUTAM Symposium on Non-Steady Flow of Water at High Speed*, Leningrad, 1971, pp. 405-426.

[35] Kato, H., "A Consideration on Scaling Laws of Cavitation Erosion," *International Shipbuilding Progress*, Vol. 22, 1975, pp. 305-327.